Molecular Plant Pathology

MOLECULAR PLANT PATHOLOGY (2018) **19**(12), 2527–2542 DOI: 10.1111/mpp.12727

Deciphering the functions of the outer membrane porin OprBXo involved in virulence, motility, exopolysaccharide production, biofilm formation and stress tolerance in *Xanthomonas oryzae* pv. *oryzae*

NAHEE BAE†, HYE-JEE PARK†, HANBI PARK, MINYOUNG KIM AND SANG-WOOK HAN*

Department of Integrative Plant Science, Chung-Ang University, Anseong, 17546, South Korea

SUMMARY

Xanthomonas oryzae pv. *oryzae* (*Xoo*) is a Gram-negative bacterium causing bacterial leaf blight disease in rice. Previously, proteomic analysis has shown that the outer membrane protein B in *Xoo* (OprBXo) is more abundant in the wildtype strain than is the outer membrane protein 1 in the *Xoo* (Omp1X) knockout mutant. OprBXo shows high homology with OprB, which has been well characterized as a carbohydrate-selective porin in *X. citri* ssp. *citri* and *Pseudomonas* species. However, the functions of OprBXo in *Xoo* have not yet been documented. To elucidate the functions of OprBXo, we generated the OprBXo-overexpressing mutant, *Xoo*(OprBXo), and the knockout mutant, *XooΔoprBXo*(EV). We found that the virulence and migration of *Xoo*(OprBXo), but not *XooΔoprBXo*(EV), were markedly reduced in rice. To postulate the mechanisms affected by OprBXo, comparative proteomic analysis was performed. Based on the results of proteomics, we employed diverse phenotypic assays to characterize the functions of OprBXo. Abnormal twitching motility and reduction in swarming motility were observed in *Xoo*(OprBXo). Moreover, *Xoo*(OprBXo) decreased, but *XooΔoprBXo*(EV) enhanced, exopolysaccharide production and biofilm formation. The chemotactic ability of *XooΔoprBXo*(EV) was dramatically lower than that of *Xoo*(EV) in the presence of glucose and xylose. *Xoo*(OprBXo) was resistant to sodium dodecylsulphate and hydrogen peroxide, but *XooΔoprBXo*(EV) was highly sensitive compared with *Xoo*(EV). Thus, OprBXo is not only essential for chemotaxis and stress tolerance, but also for motility, biofilm formation and exopolysaccharide production, which may contribute to the virulence of *Xoo*. These results will lead to new insights into the functions of a sugar-selective porin in *Xoo*.

Keywords: OprBXo, porin, proteomics, virulence, *Xanthomona oryzae* pv. *oryzae*.

*Correspondence: Email: swhan@cau.ac.kr
†These authors contributed equally to this work.

INTRODUCTION

Xanthomonas oryzae pv. *oryzae* (*Xoo*) is a Gram-negative bacterium causing bacterial leaf blight, one of the most devastating diseases affecting rice (Ronald and Leung, 2010). Bacterial blight is an economically important disease and yield losses can reach 50% (Reddy *et al.*, 2014). *Xoo* is easily disseminated from infected plants to new hosts during windy and rainy conditions, and attaches to the surface of host leaves (Nino-Liu *et al.*, 2013). The bacterium enters the host through wounds or hydathodes around the leaf tips, colonizes and spreads into the xylem vessels, resulting in the yellowing of leaves and blight symptoms (Nino-Liu *et al.*, 2013). Diseased plants start to wilt, with their colour changing to white or grey. During infection, the bacterium exploits diverse virulence factors, such as the formation of extracellular enzymes, exopolysaccharide (EPS), biofilms and type III effectors (Coplin and Cook, 2000; Das *et al.*, 2009; Malamud *et al.*, 2013).

In a previous study, we have reported that the outer membrane protein 1 in *Xoo* (Omp1X) is a porin-like protein, consisting of 10 β-sheets (Park *et al.*, 2011). Phenotypic assays have shown that Omp1X is involved in biofilm formation and motility in *Xoo*. In addition, comparative proteomic analysis for Omp1X has revealed that the expression of proteins related to motility, cell wall/membrane and signal transduction undergo remarkable changes. Among them, one of the proteins highly abundant in the wildtype is outer membrane protein B in *Xoo* (OprBXo). The deduced amino acid sequence of OprBXo shows high homology with that of the outer membrane protein B (OprB) family.

In Gram-negative bacteria, porins can selectively transport small metabolites, such as sugars, amino acids and ions. Among them, the OprB family is one of the well-characterized outer membrane porins and a selective sugar transporter (Ficarra *et al.*, 2012; Wylie and Worobec, 1995). It has been reported that glucose is selectively transported via OprB in *Pseudomonas aeruginosa* (Wylie and Worobec, 1995). Interestingly, OprB shows high uptake activity for glucose and other monosaccharides, but not for disaccharides and carboxylated glucuronates, in *Pseudomonas putida* (van den Berg, 2012). In *Xanthomonas citri*

ssp. *citri* (*Xcc*), the causal agent of citrus canker, *Xcc* OprB is also indispensable for glucose transport, and the growth of *Xcc* mutants lacking OprB is reduced in minimal medium supplemented with 0.5% glucose and sucrose as sole carbon source (Ficarra *et al.*, 2012). The OprB structure in *P. putida* and *Xcc* forms a 16-stranded β-barrel and similar hole composition, allowing assumptions in which its substrates are monosaccharides (van den Berg, 2012; Ficarra *et al.*, 2012). In *Xcc*, the OprB mutant shows a diminished virulence level, with modulation of bacterial adherence to host tissue and biofilm formation (Ficarra *et al.*, 2012). In addition, OprB is required for biofilm formation and tolerance to oxidative and detergent stress. OprB is also associated with EPS production and xanthan viscosity, affecting xanthan ingredients (Ficarra *et al.*, 2012). However, OprB function has not been characterized in *Xoo*.

Diverse experimental techniques have been employed to elucidate and postulate the functions and biological mechanisms of proteins/genes at the RNA level. In addition, proteomic analyses have been widely employed in recent years to identify the functions of proteins/genes and to check the expression profile at the protein level, in particular for specific organisms whose genomes have been established. However, the abundance of proteins is not always correlated with RNA expression because of post-transcriptional modification and regulation (Gry *et al.*, 1992). In *Xoo*, Robin *et al.* (2002) reported eight HrpX-regulated proteins by comparative proteomic analysis; however, the RNA expression of seven of these proteins was not significantly altered (Robin *et al.*, 2002), indicating that the expression patterns of RNA and proteins are not always consistent in *Xoo*. Therefore, comparative proteomic analysis is a pivotal tool to predict the functions of proteins and their related cellular mechanisms at the protein level.

Here, we report the functions of OprBXo (Accession No. MF521484) by generating the OprBXo knockout mutant, *XooΔoprBXo*, as well as the OprBXo-overexpressing mutant, *Xoo*(OprBXo). To postulate the biological and cellular functions associated with OprBXo, the patterns of protein expression in *Xoo*(OprBXo) and *XooΔoprBXo* were compared with those in the wildtype by label-free shotgun proteomic analysis and classification of clusters of orthologous groups (COGs). On the basis of the proteomic results, we carried out diverse phenotypic assays. Proteomic and phenotypic characterization revealed that OprBXo is involved in virulence, motility, EPS production, biofilm formation, chemotaxis and stress tolerance in *Xoo*.

RESULTS

OprBXo is a porin-like protein

OprBXo possesses high homology with OprB (Fig. 1A) from *Xcc* and *P. putida* F1, which are known to be carbohydrate-selective porins (van den Berg, 2012; Ficarra *et al.*, 2012). The deduced amino acid sequence of OprBXo shows 85% (361/423) identity with *Xcc* OprB, and *P. putida* F1 OprB (F1-OprB) shows 30% (126/423) identity with OprBXo. It is known that loop L2, governing substrate specificity and forming a pore, is unique to the OprB family (van den Berg, 2012). L2 of OprBXo is identical with the same region of *Xcc* OprB and shows 65% identity with that of *P. putida* (Fig. 1A), suggesting that OprBXo is also a carbohydrate-selective porin. To study the structure of OprBXo, the predicted three-dimensional structure of OprBXo was generated using the I-TASSER server and PyMOL program (Fig. 1B). The putative structure of OprBXo formed a β-barrel consisting of 16 β-sheets, similar to OprB from *Xcc* and *P. putida* F1. In addition to the β-barrel structure, the porin family contains an N-terminal signal peptide for localization on the outer membrane (Park *et al.*, 2011). A prediction using SignalP 4.1 (Petersen *et al.*, 2016) showed that OprBXo also possesses a putative signal peptide on the N-terminus (Fig. 1C), indicating that OprBXo should localize at the outer membrane in *Xoo*.

Overexpression of OprBXo reduces virulence and migration of *Xoo*

In *Xcc*, OprB is involved in virulence and bacterial growth in host leaves (Ficarra *et al.*, 2012). Hence, we examined the effect of OprBXo on virulence in rice plants (Fig. 2). After inoculation of the four strains, *Xoo*(EV), *Xoo*(OprBXo), *XooΔoprBXo*(EV) and *XooΔoprBXo*(OprBXo), the lesion length was measured at 0, 3, 6, 9, 12 and 15 days after inoculation (DAI). *Xoo*(EV) and *XooΔoprBXo*(EV) represent the wildtype and *XooΔoprBXo* strain carrying an empty vector (EV), respectively. *XooΔoprBXo*(OprBXo) and *Xoo*(OprBXo) denote *XooΔoprBXo* and the wildtype strain transformed with the OprBXo overexpression vector. *oprBXo* expression in *XooΔoprBXo*(OprBXo) and *Xoo*(OprBXo) was compared by quantitative real-time polymerase chain reaction (qPCR). Overall, the expression levels of the *oprBXo* gene were statistically lower in *XooΔoprBXo*(OprBXo) than in *Xoo*(OprBXo) (Fig. S1, see Supporting Information). Interestingly, the OprBXo-overexpressing strain, *Xoo*(OprBXo), showed significantly reduced lesion length, but *XooΔoprBXo*(EV) and *XooΔoprBXo*(OprBXo) were similar to *Xoo*(EV) (Fig. 2A,B). However, the *Xoo*(OprBXo) population in the infected leaves was comparable with that in *Xoo*(EV) (Fig. 2C). Therefore, the infected leaves were divided into five sections (I–V), and the bacterial population in these sections was established to investigate migration in infected leaves at 15 DAI. The patterns of *Xoo*(OprBXo) were clearly distinct from those of the other three strains, *Xoo*(EV), *XooΔoprBXo*(EV) and *XooΔoprBXo*(OprBXo) (Fig. 2C). The bacterial number in *Xoo*(OprBXo) was significantly higher (>100-fold) than that in the other three strains in section I. The patterns of the bacterial population in sections II and III were also similar to that in section I. However, the *Xoo*(OprBXo)

A

```
OprBXo       ------------------MTALAPRRARTRLLCLSLTLALTPLAHAQDATDAFKLKLGYT 42
XccOprB      ------------------------------------------------------------
F1OprB_1     MEQRKRIKTLGSLALLALVGSSGTQAAEAFSSESKWMTGDWGGTRTELLDKGYDFTLDYV 60

OprBXo       GEAASMIDGGRKSG--DAYAGQLMVG-TDVMDRLFGWNGATVKLYVTNRHGTNLANSSIG 99
XccOpr       -----MIDGGRKSG--DAYAGQLMVGTDVDMDRLFGWNGATVKLYVTNRHGTNLANSSIG 53
F1OprB_1     GEVAGNLHGGYNDDKTARYSDQFALGAHLDLQKILGWHDAEFKLAITERSGRNLSNDRIS 120
                    :.** :..    *:.*: :*    :::::**:.* .** :*:* * **:*. *.
OprBXo       N-----STSVQEIYG-GQGTRLTNFTLLQKLFNDRLELEAGRSVANIHFLGSDLCQYFQG 153
XccOprB      N-----STSVQEIYG-GQGTRLANFTLLQKLFNDRLELEAGRSVANIHFLGSDLCQYFQG 107
F1OprB_1     DPRAGQFSSVQEVWGRGQTWRLTQMWIKQKYFDGALDVKFGRFGEGEDFN-SFPCD-FQN 178
             :      :****::* **  **::: : ** *:. *::: **   . .*  *  *: **.
OprBXo       NSACGNPTFVFRTSNFTYWPVSSWAADATAWVTPKVYVHVGAYEVNPVQAQDGQHGLNWS 213
XccOprB      NSACGNPTFVFRTSNFTYWPVSSWAAHATAWVTPKVYLHVGAYEVNPIQAQDGQHGLNWS 167
F1OprB_1     LAFCGSQVGNWVGGIWYNWPVSQWALRVKYNITPAFFVQVGAFEQNPSNLETG-NGFKLS 237
              : **. .  :  . :  ****.**  ..  :** .:::***:* ** : : * :*:: *
OprBXo       TNDTTGVVVP-AVGYKNKGGDGSMAAMYELGGWQDNSDYTDPLRDRNGNPAVLSGLPYGN 272
XccOprB      TNDTTGVVVPYAVGYKNKGGDGSMAAMYELGGWQDNSDYSDPLRDRNGNPAVLSGLAYEN 207
F1OprB_1     GSGTKGAILPVEAVWSPKVN--GLPGEYRLGYYYSTAKADDVYDDVNGNPQALTGEAFKS 295
              ..*.*.::*  . :. * .  .:.. *.** : ..:.  *   * **** .*:* .: .
OprBXo       KQGRSGLFARFEQQVTNPDPSSTRGLTVFGAILQSTSGQAIEDHFVQLGLVQKGTFASRP 332
XccOprB      KQGRSGLFARFEQQVTNPDPSGTRGLTVFGAVLQSTGGQAIEDHFIQLGLVQKGTFASRP 267
F1OprB_1     HSSKHGWWVVAQQQVTAHGGDVNRGLSLFANFTVHDKATNVVDNYQQVGLVYKGAFDARP 355
             :..: * :.  :****  . . .***::*. .  : *:: *:*** **:* :**    **
OprBXo       QDNIAFVITQQKYSDQAIENLRLARASAGGTGTP-------ADNQIMMELSYGIQVTKQL 385
XccOprB      QDNIAFVITQQKYSDEAIENLRLARASAGGTGTP-------ADNQIMMELSYGIQVTKRL 320
F1OprB_1     KDDIGFGVARIHVNDDVKKRAELLNAQSGINDYDNPGFVPLQRTEYNAELYYGFHVTNWL 415
             :*:*.* ::: : .*:. :. .* .*.:* ..           .:   ** **::**: *
OprBXo       RIAPNLHYVINPDQFNEPTRTNDLKNALIAGLRIDWNL 423
XccOprB      RIAPNLHYVINPDQFNEPTRTTDLKNALIAGMRIDWNL 378
F1OprB_1     TVRPNLQYIKSPG------GVDEVDNALVAGLKIQSSF 447
              : ***:*: .*.       . ::.***:**::*: .:
```

B

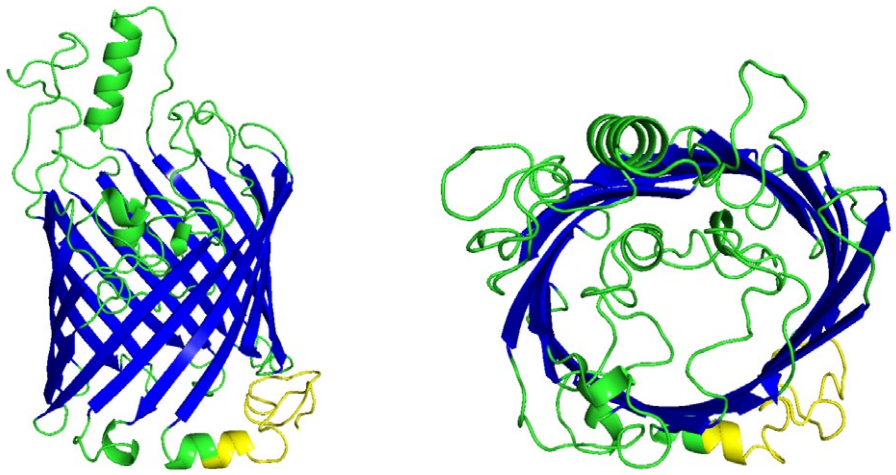

C

MTALAPRRARTRLLCLSLTLALTPLAHAQDATDAFKLKLGYTGEAASMIDGGRKSGDA
YAGQLMVGTDVMDRLFGWNGATVKLYVTNRHGTNLANSSIGNSTSVQEIYGGQGTR
LTNFTLLQKLFNDRLELEAGRSVANIHFLGSDLCQYFQGNSACGNPTFVFRTSNFTY
WPVSSWAADATAWVTPKVYVHVGAYEVNPVQAQDGQHGLNWSTNDTTGVVVPAV
GYKNKGGDGSMAAMYELGGWQDNSDYTDPLRDRNGNPAVLSGLPYGNKQGRSGL
FARFEQQVTNPDPSSTRGLTVFGAILQSTSGQAIEDHFVQLGLVQKGTFASRPQDNIA
FVITQQKYSDQAIENLRLARASAGGTGTPADNQIMMELSYGIQVTKQLRIAPNLHYVIN
PDQFNEPTRTNDLKNALIAGLRIDWNL

Fig. 1 Sequence alignment and the predicted three-dimensional structure of OprBXo. (A) Sequences of OprBXo, *Xcc* OprB from *Xanthomonas citri* ssp. *citri* and F1OprB_1 from *Pseudomonas putida* F1 were compared using the CLUSTALW program. '*', ':' and '.' indicate identical residues, conserved substitutions and semi-conserved substitutions, respectively. A red box reveals a putative loop L2 region. The red letters represent residues critical for interaction with substrates. (B) Predicted three-dimensional structures were produced by the PyMOL program. (C) Amino acid sequences of OprBXo. Blue and yellow indicate putative β-strands and the predicted signal peptide, respectively. [Colour figure can be viewed at wileyonlinelibrary.com]

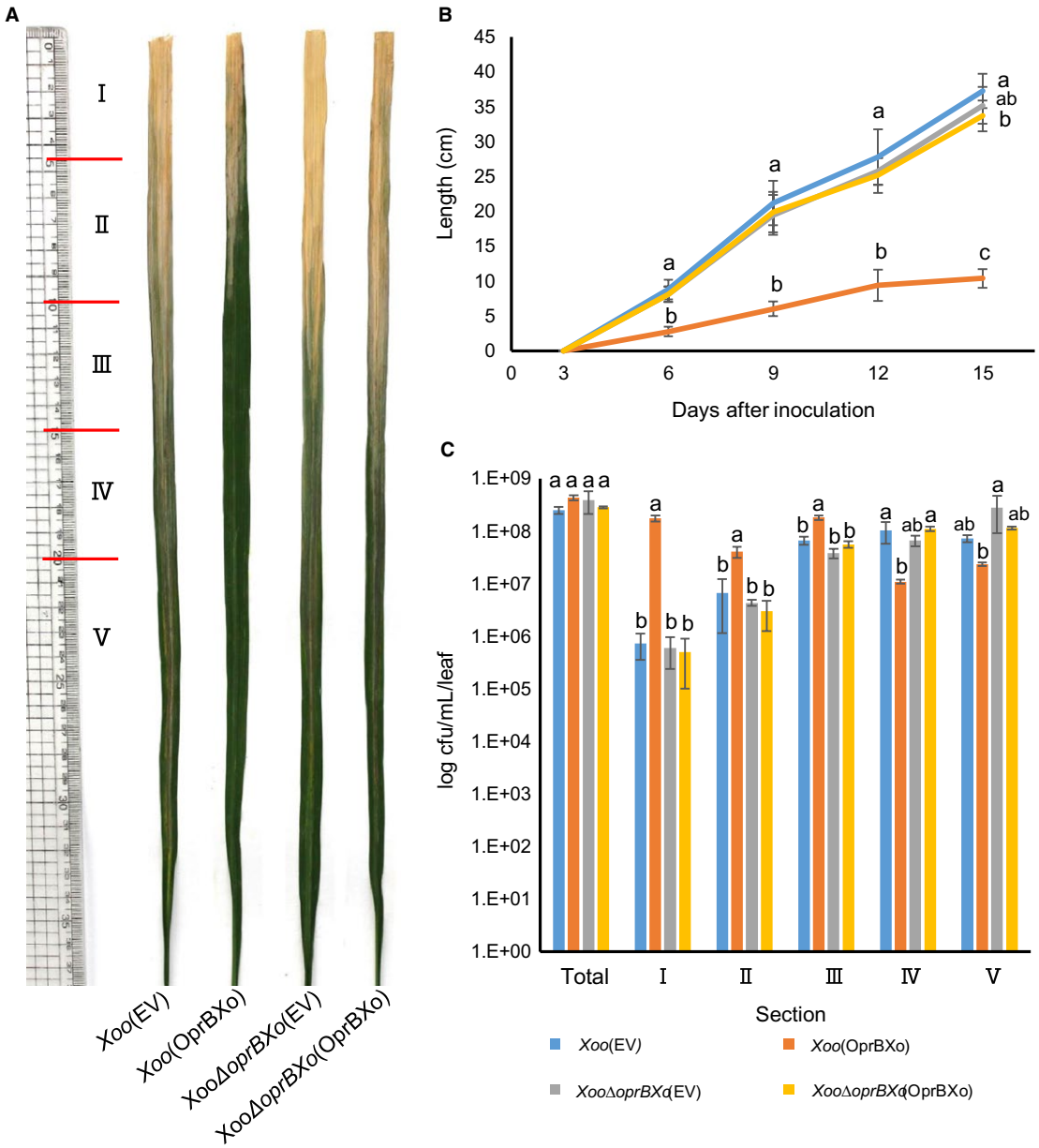

Fig. 2 Virulence assay for *Xoo*(EV), *Xoo*(OprBXo), *XooΔoprBXo*(EV) and *XooΔoprBXo*(OprBXo). (A) Water-soaked lesions from inoculated leaves at 15 days after inoculation (DAI). (B) Lesion length development in diseased leaves infected by the four strains during 15 days. (C) Bacterial population in the infected leaves at 15 DAI. The *Xanthomonas oryzae* pv. *oryzae* (*Xoo*) strain suspensions were adjusted to an optical density at 600 nm ($OD_{600\,nm}$) of 0.6 in 10 mM $MgCl_2$, and then inoculated onto Kitaake leaves by the scissor clipping method. Bacterial cells were recovered from each section: I (0–5 cm), II (6–10 cm), III (11–15 cm), IV (16–20 cm) and V (>21 cm). After serial dilution, cells were enumerated by a colony counting method. The bars in the graphs represent the mean of at least nine leaves with standard deviations. Different letters on the bars indicate statistically significant differences by one-way analysis of variance (ANOVA) ($P < 0.05$). cfu, colony-forming unit. This experiment was repeated at least five times. [Colour figure can be viewed at wileyonlinelibrary.com]

population was much lower than that in the other strains in sections IV and V, suggesting that *Xoo*(OprBXo) mainly colonized the upper part of infected leaves. These results indicate that OprBXo is involved in the migration of *Xoo* in infected leaves, which may contribute to optimal virulence in the host.

Comparative proteomic analysis of OprBXo

Proteomic analysis is a useful tool for the prediction of proteins/genes at the protein level, but the expression of proteins related to OprB has not been reported to date. Therefore, proteomic analysis was performed to decipher the functions of OprBXo

involved in virulence and other biological processes in *Xoo*. The abundance of proteins in *Xoo*(OprBXo) and *XooΔoprBXo* was compared with that in *Xoo*(EV) and *Xoo*, respectively, by label-free shotgun proteomics combined with COGs analysis. XOM2, which is a synthetic, minimal and plant-mimic medium (Wengelnik *et al*., 1996), was used for proteomic analysis because the involvement of OprBXo in optimal virulence is obvious.

The proteins and peptide spectral matches (PSMs) detected from three biological replicates of *Xoo*(EV) and *Xoo*(OprBXo) are described in Table S1 (see Supporting Information). Among the proteins detected in the liquid chromatography-tandem mass spectrometry (LC-MS/MS) experiment, 1291 and 1126 proteins were shared in the three replicates of *Xoo*(EV) and *Xoo*(OprBXo), respectively, and the proteins were used for comparison (Table S1). Three hundred and eighty-four and 139 proteins were more abundant (more than two-fold) in *Xoo*(EV) and *Xoo*(OprBXo), respectively (Tables S2 and S3, see Supporting Information). These differentially abundant proteins were subjected to COGs analysis. Except for group P (inorganic ion transport and metabolism), the number of proteins detected from *Xoo*(EV) was higher than that from *Xoo*(OprBXo) in most categories of COGs (Fig. 3A). The abundance of proteins belonging to groups E (energy production and conversion), G (carbohydrate metabolism and transport), M (cell wall/membrane/envelop biogenesis) and T (signal transduction) was highly affected by OprBXo. Interestingly, 11 type III effectors (XopF1, XopK, XopQ, XopR, XopW, XopV, XopX, Hpa3, PthXo1, TalC3a and Tal5b) were abundant in *Xoo*(EV), but none were detected in *Xoo*(OprBXo) (Tables S2 and S3). In addition, eight Gum proteins (GumB, GumC, GumH, GumI, GumJ, GumK, GumM and GumN), which are related to EPS production, and six clustered regularly interspaced short palindromic repeats (CRISPR)/CRISPR associated protein (CAS) proteins (Cas1, Cas3, Cas4, Cas5, Csd1 and Csd2) were highly expressed in *Xoo*(EV) (Table S2).

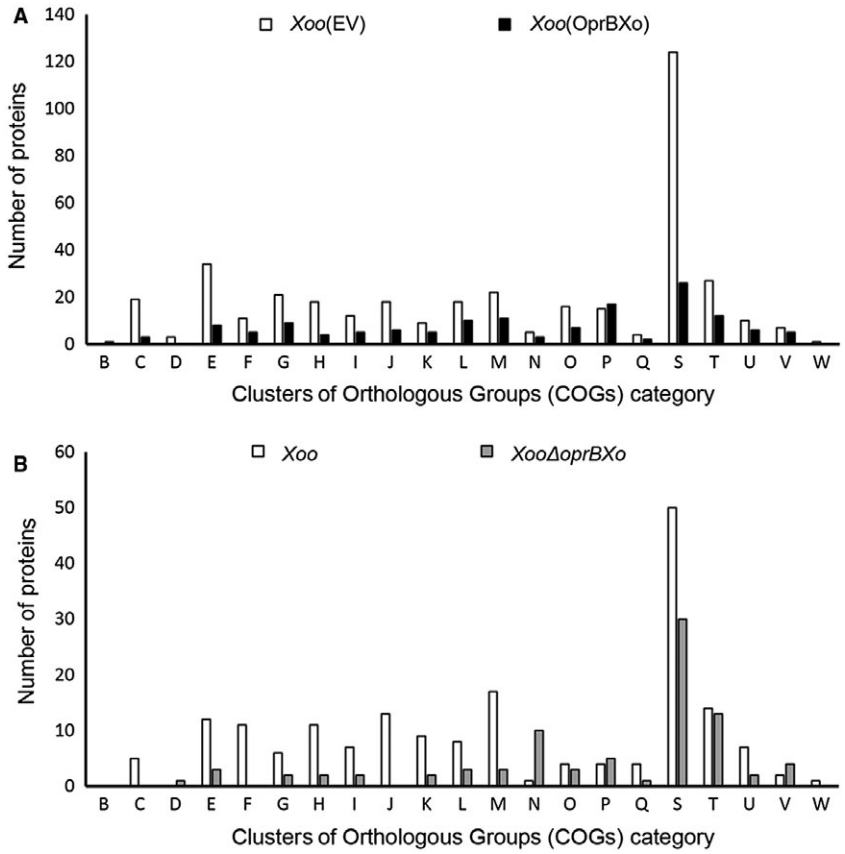

Fig. 3 Clusters of orthologous groups (COGs) of proteins regulated by OprBXo. (A) Bar graphs represent the COGs classification of 384 and 139 proteins, which were abundant (more than two-fold) in *Xoo*(EV) and *Xoo*(OprBXo), respectively. (B) COGs analysis of 181 and 80 proteins, which were highly expressed (more than two-fold) in *Xanthomonas oryzae* pv. *oryzae* (*Xoo*) and *XooΔoprBXo*, respectively. Groups: B, chromatin structure and dynamics; C, energy production and conversion; D, cell cycle control and mitosis; E, amino acid metabolism and transport; F, nucleotide metabolism and transport; G, carbohydrate metabolism and transport; H, coenzyme metabolism; I, lipid metabolism; J, translation; K, transcription; L, replication and repair; M, cell wall/membrane/envelop biogenesis; N, cell motility; O, post-translational modification, protein turnover, chaperone functions; P, inorganic ion transport and metabolism; Q, secondary structure; R, general functional prediction only; S, function unknown; T, signal transduction; U, intracellular trafficking and secretion; V, defence mechanisms.

Next, we carried out comparative proteomic analysis between *Xoo* and *XooΔoprBXo*; 1227 and 1113 proteins were commonly found in three biological replicates of *Xoo* and *XooΔoprBXo*, respectively (Table S4, see Supporting Information). Among these proteins, 181 and 80 proteins, which were highly expressed (more than two-fold) in *Xoo* and *XooΔoprBXo*, respectively, were used for COGs analysis (Tables S5 and S6, see Supporting Information). Proteins belonging to the N group (motility) were highly abundant in *XooΔoprBXo* compared with the wildtype (Fig. 3B). Interestingly, 11 chemotaxis-related proteins, mostly categorized in the N (motility) and T (signal transduction) groups, were highly expressed in *XooΔoprBXo*, but only one protein was observed in *Xoo* (Tables S5 and S6). In addition, four type III effectors (Hpa1, TalC2a, TalC4 and TalC9e) were more abundant in *XooΔoprBXo* compared with the wildtype (Table S6).

OprBXo is related to EPS production and biofilm formation

Proteomic analyses clearly showed that OprBXo might be associated with the expression of Gum proteins. In addition, *Xcc* OprB is involved in EPS production and xanthan biosynthesis (Ficarra *et al.*, 2012). Therefore, we examined the production of EPS, which is a major component of xanthan, by the four strains (Fig. 4A). *Xoo*(OprBXo) and *XooΔoprBXo*(EV) showed an opposite pattern. The production of EPS was reduced (1.5-fold) in *Xoo*(OprBXo), but was markedly higher in *XooΔoprBXo*(EV) (1.9-fold), compared with that in *Xoo*(EV). The complemented strain could restore the function, similar to *Xoo*(EV), indicating the absence of a polar effect. When the bacterial cells attach to the surface, they produce EPS, assemble themselves and form biofilms (Sutherland, 2001). Thus,

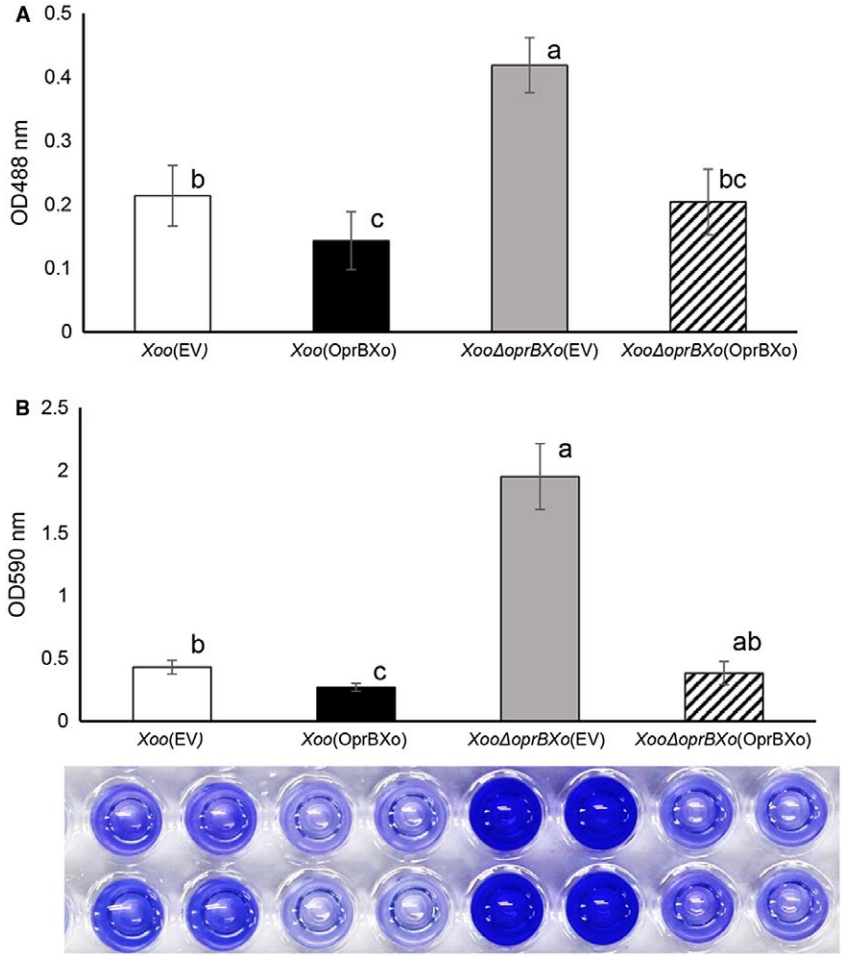

Fig. 4 Exopolysaccharide (EPS) production and biofilm formation by *Xoo*(EV), *Xoo*(OprBXo), *XooΔoprBXo*(EV) and *XooΔoprBXo*(OprBXo). (A) Quantification of EPS production by the four strains. After the *Xanthomonas oryzae* pv. *oryzae* (*Xoo*) strains had been incubated in PSB for 5 days, EPS was extracted and quantified by the phenol–sulphuric acid method using a UV spectrophotometer at 488 nm. Bars in the graph represent the mean of three biological replicates, with standard deviation. (B) Biofilm formation by *Xoo* strains. The four strains were incubated in a 96-well polyvinyl chloride plate for 7 days, and biofilm formation was quantified by the crystal violet staining method using a UV spectrophotometer at 590 nm. Images were captured at day 7. Bars in the graph represent the mean of 16 biological replicates, with standard deviation. Different letters on the bars indicate statistically significant differences observed by one-way analysis of variance (ANOVA) ($P < 0.05$). This experiment was repeated at least six times. [Colour figure can be viewed at wileyonlinelibrary.com]

EPS production is closely related to biofilm formation. To assess whether OprBXo was also involved in biofilm formation, a 96-well polyvinyl chloride (PVC) plate adherence assay was carried out. The pattern of biofilm formation from the four strains was similar to that of EPS production (Fig. 4B). Biofilm formation by *Xoo*(OprBXo) was decreased (1.6-fold) compared with that of *Xoo*(EV). However, biofilm formation by *XooΔoprBXo* was significantly enhanced (4.1-fold); the complemented strain could reinstate biofilm formation. These results clearly demonstrate that OprBXo plays a pivotal role in EPS production and biofilm formation.

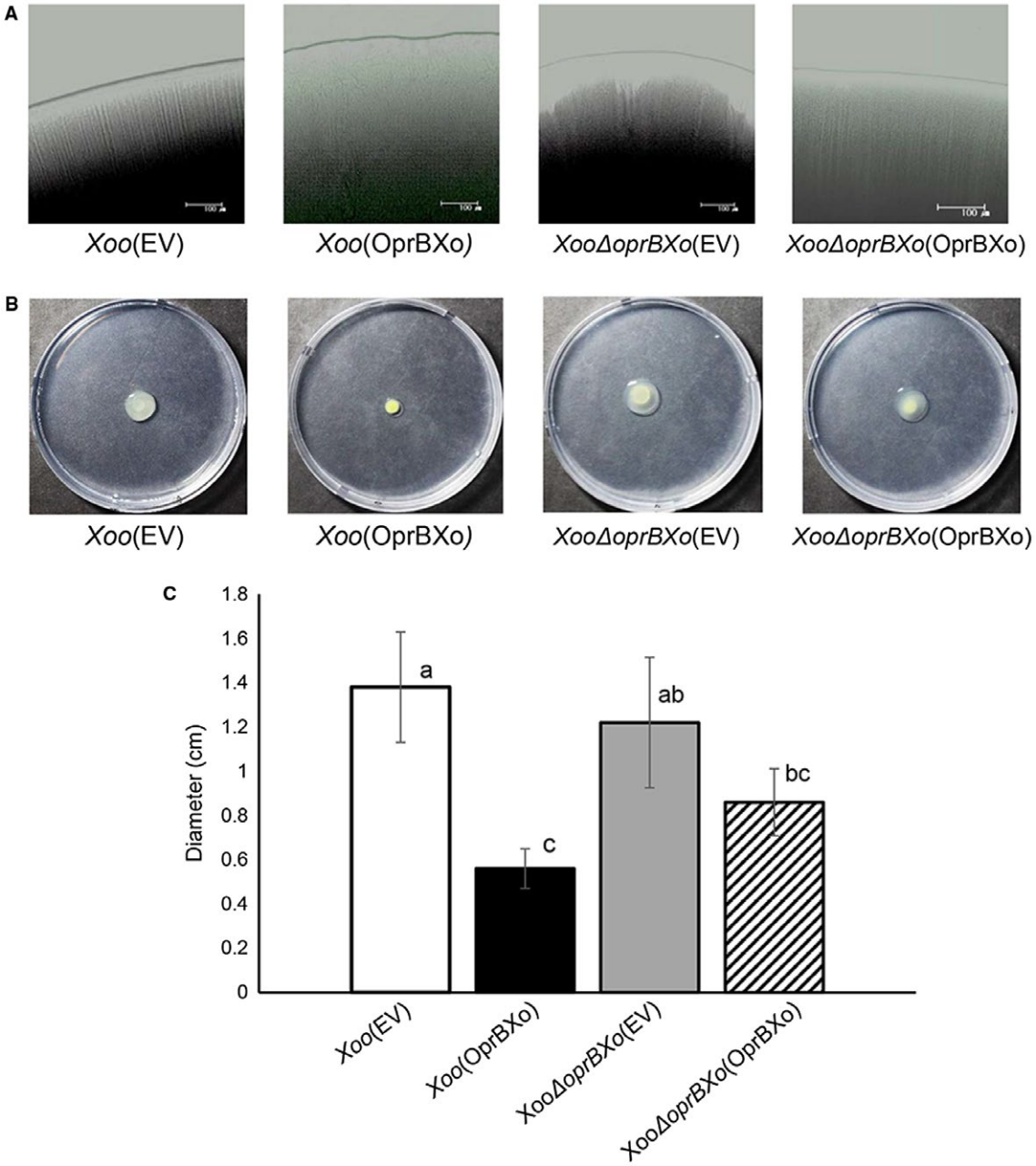

Fig. 5 Twitching and swarming motility of *Xoo*(EV), *Xoo*(OprBXo), *XooΔoprBXo*(EV) and *XooΔoprBXo*(OprBXo). (A) Twitching motility of *Xanthomonas oryzae* pv. *oryzae* (*Xoo*) strains. Approximately 3 μL of bacterial suspension [optical density at 600 nm ($OD_{600\ nm}$) of 0.6] were spotted on PSA and incubated for 3 days. The formation of marginal fringes was observed using a light microscope. Bars represent 100 μm. (B, C) Swarming motility of *Xoo* strains on XOM2 medium. The diameter of the colony expansion zone was measured, and images were captured at 7 days after incubation. Bars in the graph represent the mean of five biological replicates, with standard deviation. Different letters on the bars indicate statistically significant differences by one-way analysis of variance (ANOVA) ($P < 0.05$). This experiment was repeated at least six times. [Colour figure can be viewed at wileyonlinelibrary.com]

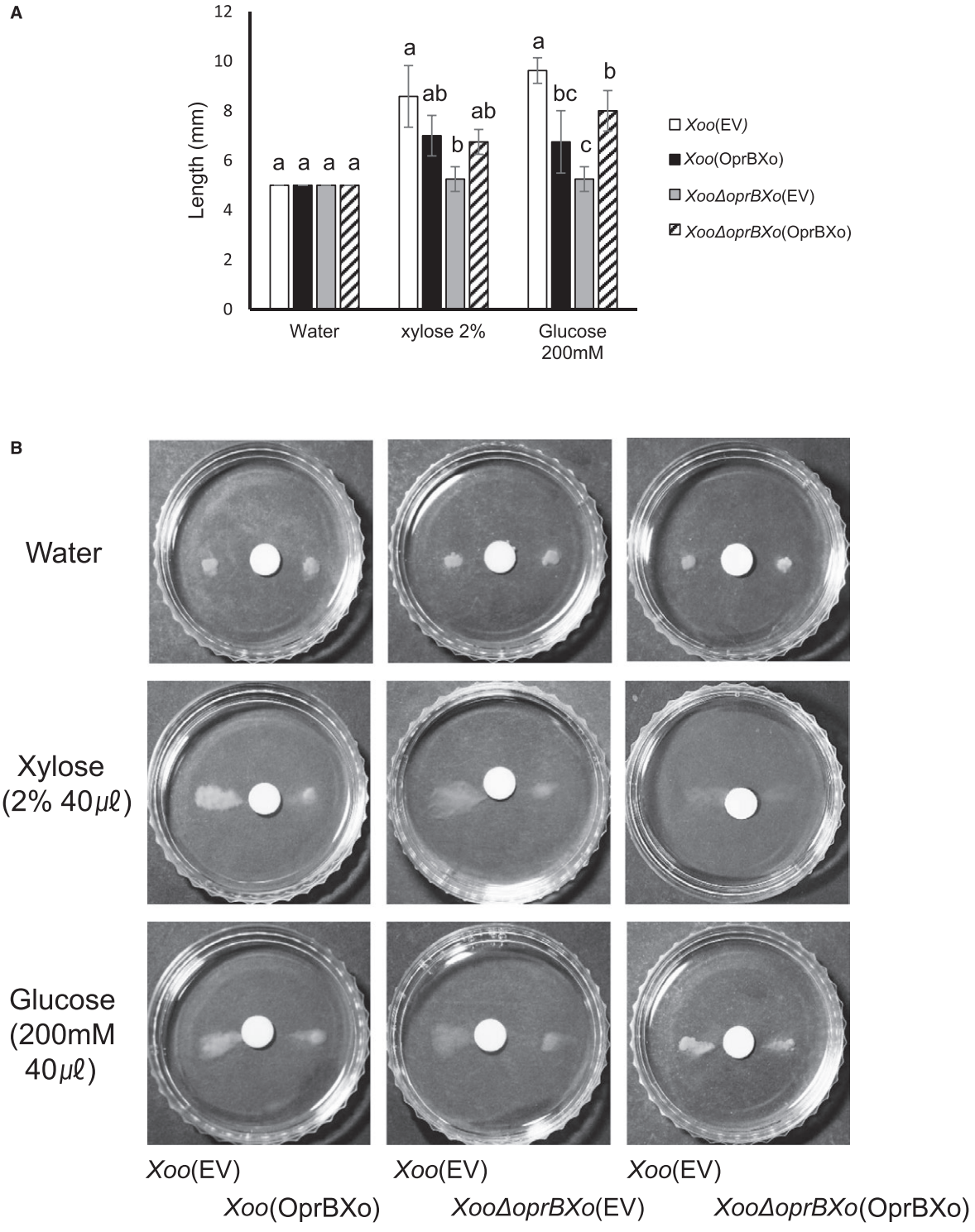

Fig. 6 Chemotaxis assay in *Xoo*(EV), *Xoo*(OprBXo), *XooΔoprBXo*(EV) and *XooΔoprBXo*(OprBXo). (A) Quantification of the distance by measuring the chemotactic ability of the four strains. Paper discs soaked in 2% xylose, 200 mM glucose or water were placed at the centre of the plates containing 1% hypromellose without any carbon source. *Xanthomonas oryzae* pv. *oryzae* (*Xoo*) strain suspension was inoculated 1 cm away from the discs, followed by 1 day of incubation. Bars represent the mean of four independent experiments, with standard error. Different letters on the bars indicate statistically significant differences observed by one-way analysis of variance (ANOVA) ($P < 0.05$). (B) Representative images captured 1 day after incubation. To the left is *Xoo*(EV) and to the right is *Xoo*(OprBXo), *XooΔoprBXo*(EV) or *XooΔoprBXo*(OprBXo). This experiment was repeated at least three times.

OprBXo is required for twitching and swarming motility

Because *Xoo*(OprBXo) reduced migration in infected leaves and proteomic analyses revealed that the abundance of proteins related to motility was influenced by OprBXo, we investigated the role of OprBXo in motility. For twitching motility, *Xoo* strains were grown on peptone sucrose agar (PSA) plates, and the edges of the colonies were observed using a light microscope (Fig. 5A). *Xoo*(EV) showed many vertical and fine lines in order, but *Xoo*(OprBXo) displayed no lines and was severely irregular. *XooΔoprBXo*(EV) also showed very irregular abnormal shapes that had no sequential fine lines. The complemented strain, *XooΔoprBXo*(OprBXo), restored the twitching function to that of *Xoo*(EV). To determine the swarming motility, *Xoo* strains were incubated on semi-solid plates containing 0.3% agar for 7 days, and the diameter was measured (Fig. 5B,C). The swarming function of *Xoo*(OprBXo) was impaired, and no obvious differences were observed between *XooΔoprBXo*(EV) and *Xoo*(EV). These data demonstrate that OprBXo is required for optimal motility in *Xoo*.

OprBXo is required for chemotaxis

Proteomic analysis showed that the expression of diverse chemotaxis-related proteins was affected by OprBXo, and the OprB family is known to be a glucose-selective porin family in other Gram-negative bacteria. Therefore, we tested whether OprBXo is involved in *Xoo* chemotaxis using a disc assay. In addition to glucose, we used xylose as a chemoattractant because the expression of chemotaxis-related proteins was altered in XOM2, which contains xylose as a carbon source (Fig. 6). None of the strains migrated towards water. Interestingly, *XooΔoprBXo*(EV) was not attracted to glucose and xylose, compared with *Xoo*(EV), and *XooΔoprBXo*(OprBXo) restored its chemotactic function to the level of *Xoo*(EV) (Fig. 6), thus showing that OprBXo is also a carbohydrate-selective porin. In the strain overexpressing OprBXo, slightly reduced chemotactic activity was also observed, and impaired motility of *Xoo*(OprBXo) could be one of the reasons for the retarded chemotactic activity in this strain.

OprBXo is essential for tolerance to sodium dodecylsulphate (SDS) and hydrogen peroxide (H_2O_2)

Comparative proteomic analyses revealed that the abundance of proteins belonging to the M group (cell wall/membrane/envelope) was significantly altered (Fig. 3). The bacterial cell wall/membrane/envelope possesses a significant role in protection against diverse environmental stresses (Raivio, 2012). Therefore, we further investigated the role of OprBXo in the tolerance to H_2O_2 and SDS. *Xoo* strains were incubated in peptone sucrose broth (PSB) at 10^5 colony-forming units (cfu)/mL with 0.001% SDS or 0.05 mM H_2O_2. Cell viability was measured by counting the colonies on the plates. The response of the test strains to SDS and H_2O_2 showed similar patterns (Fig. 7). Although *Xoo*(OprBXo) was more resistant to both SDS and H_2O_2, *XooΔoprBXo*(EV) was significantly more sensitive to SDS and H_2O_2, compared with *Xoo*(EV). In addition, *XooΔoprBXo*(OprBXo) successfully restored its tolerance to the level shown by *Xoo*(EV). Combined with proteomic analysis, these data demonstrate that OprBXo is indeed involved in cell membrane/envelope function.

The relationship between Omp1X and OprBXo

The expression of OprBXo influenced by Omp1X has been demonstrated in a previous proteomic analysis (Park *et al.*, 2011). To support the proteomic results, transcripts of the *oprBXo* gene were evaluated in *Xoo* and *XooΔom1X* by qPCR using two OprBXo-specific primers (Fig. S2, see Supporting Information). To enhance the reliability, we used total RNA from two strains harvested at an optical density at 600 nm ($OD_{600\ nm}$) of 0.06, 0.6 and 1.5. Expression levels of the *oprBXo* gene in *XooΔomp1X* were much lower than those in *Xoo* in all given conditions (Fig. S2), indicating that the expression of OprBXo is positively regulated by Omp1X. Bahar *et al.* (2014) have reported that Omp1X is secreted into the culture supernatants with outer membrane vesicles (OMVs) in *Xoo*. Therefore, we also investigated whether OprBXo is secreted into supernatants in *Xoo*(OprBXo). Using anti-6×His for OprBXo and anti-Omp1X antibodies, immunoblot analysis was performed (Fig. S3, see Supporting Information). Unlike Omp1X, the recombinant OprBXo was only detected in total cell extracts, but not in culture supernatants from *Xoo*(OprBXo) (Fig. S3). It seems that the recombinant OprBXo is not secreted into culture supernatants in the given conditions, although there is still a possibility that the native OprBXo is secreted.

DISCUSSION

In Gram-negative bacteria, outer membrane porins are involved in various functions, such as small molecule uptake, membrane stability, motility, biofilm formation, virulence and protein/gene expression (Koebnik *et al.*, 1995; Noinaj *et al.*, 2014a). Porins consist of even numbers of β-strands, ranging from eight to 22 (Schulz, 2000). Previously, we have reported that Omp1X possesses putatively 10 β-strands consisting of a barrel shape (Park *et al.*, 2011). The putative structure of OprBXo represents 16 β-strands and also forms a barrel shape. However, there is no homology between Omp1X and OprBXo. The structural difference suggests that they may possess distinct functions in *Xoo.* However, their roles may be related, because Omp1X is positively involved in the expression of OprBXo at the protein (Park *et al.*, 2011) and RNA (Fig. S2) levels.

Although a positive relationship was shown between Omp1X and OprBXo expression and both are involved in biofilm formation in *Xoo*, *XooΔomp1X* showed reduced biofilm formation (Park *et al.*, 2011), but *XooΔoprBXo* displayed an enhanced

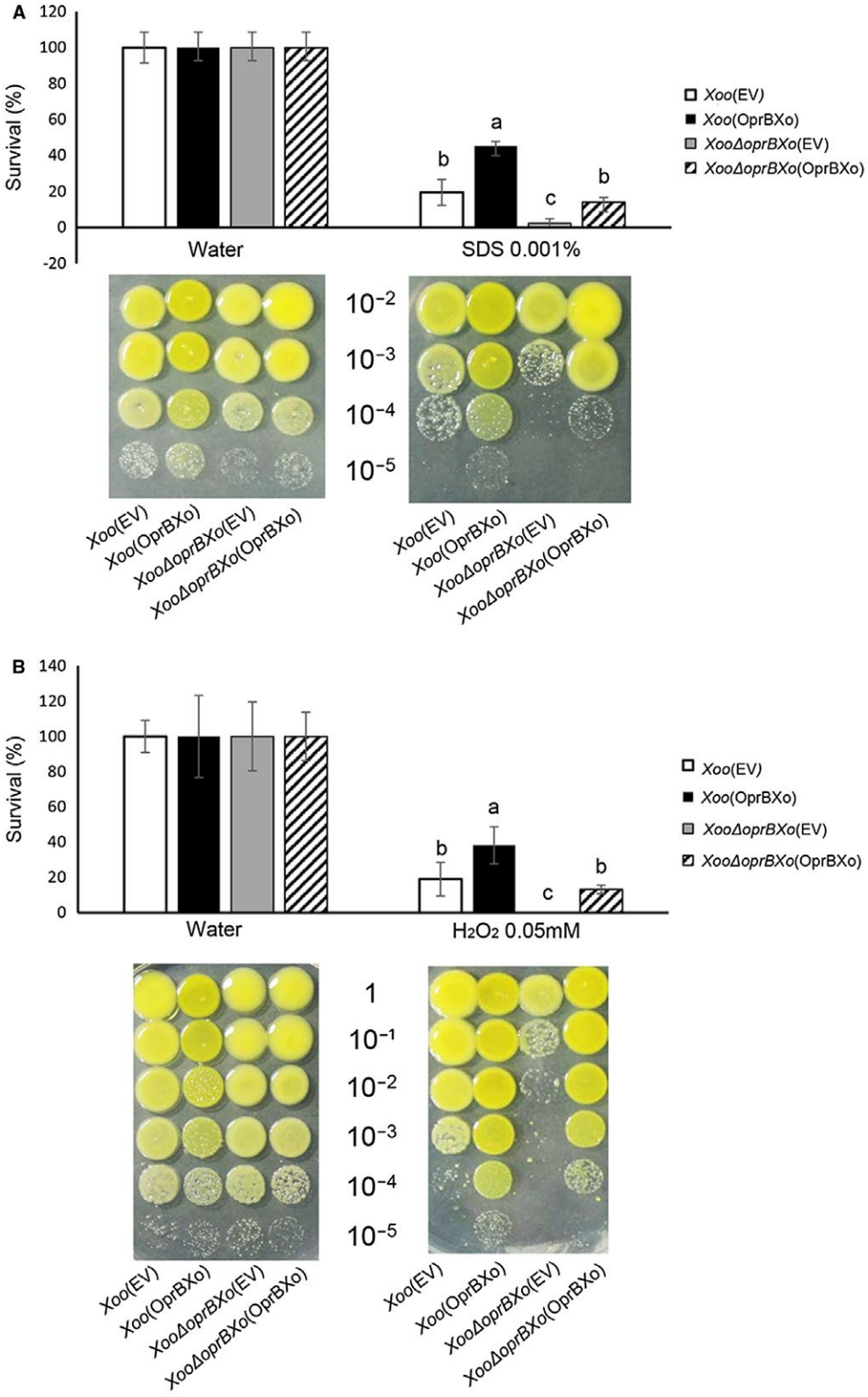

Fig. 7 Tolerance of *Xoo*(EV), *Xoo*(OprBXo), *XooΔoprBXo*(EV) and *XooΔoprBXo*(OprBXo) to sodium dodecylsulphate (SDS) and hydrogen peroxide (H_2O_2), shown in terms of the survival rate of the four strains in SDS (A) and H_2O_2 (B). *Xanthomonas oryzae* pv. *oryzae* (*Xoo*) strains were diluted to an optical density at 600 nm ($OD_{600\ nm}$) of 0.3 and cultured in PSB containing 0.001% SDS, 0.05 mM H_2O_2 or water for 24 h. Bacterial cells were enumerated by a colony counting method. Each bar represents the mean of three independent replicates, with standard deviation. Different letters on the bars indicate statistically significant differences observed by one-way analysis of variance (ANOVA) ($P < 0.05$). This experiment was repeated at least five times. [Colour figure can be viewed at wileyonlinelibrary.com]

ability to form biofilms (Fig. 4B). It is well known that diverse factors, including cell motility and EPS production, are associated with biofilm formation (Danese *et al.*, 2009; Malamud *et al.*, 2002; Mattick, 2016). In a previous study, the expression of proteins related to flagella and pili was positively regulated by Omp1X in a proteomic analysis and *XooΔomp1X* showed reduced flagella-dependent motility (Park *et al.*, 2011). However, the abundance of proteins belonging to cell motility was much higher in *XooΔoprBXo* than in the wildtype (Fig. 3A), and *XooΔoprBXo*(EV) did not alter the function of flagella-dependent motility (Fig. 5B). In addition, EPS production in *XooΔoprBXo*(EV) was enhanced (Fig. 4A). These observations may explain the different ability to form biofilms in *XooΔomp1X* and *XooΔoprBXo*.

It is also known that Omp1X is found in OMVs from culture supernatants of *Xoo* and from quorum sensing (QS) in *Stenotrophomonas maltophilia*, suggesting that Omp1X should be secreted to mediate QS (Bahar *et al.*, 2014; Devos *et al.*, 1999). In immunoblot analysis, recombinant OprBXo was not detected in culture supernatants (Fig. S3), although both OprBXo and Omp1X belong to the porin family and the expression of OprBXo was affected by Omp1X at the protein (Park *et al.*, 2011) and RNA (Fig. S2) levels. Therefore, it can be postulated that OprBXo is mainly located at the outer membrane in living cells, rather than in cell-free culture supernatants, because OprBXo is involved in the transport of glucose and xylose (Fig. 6), which can be used as carbon sources within *Xoo* for growth.

In this study, we showed that OprBXo shares homology with OprB proteins in *Xcc* and *P. putida*, possessing 16 β-strands and sugar-selective porins. Loop L2 is indispensable for stability in major porins and is important for substrate specificity to promote carbohydrate binding (van den Berg, 2012). Porins possessing 16 β-strands form a trimeric structure with extracytoplasmic loops, and are generally known as non-specific porins (Galdiero *et al.*, 2009). In addition, the β-strands of these porins are highly conserved, but there are variations in the loop regions that are indispensable for the recognition of specific substrates. Members of the OprB family are carbohydrate porins; the L2 loop region in the OprB family is highly conserved (Fig. 1A). The Arg^{88}, Gln^{105}, Glu^{106} and Gly^{109} residues in L2, which are the conserved residues in *Pseudomonas* spp. and are essential for interaction with specific substrates (van den Berg, 2012), are also conserved in OprBXo, as well as *Xcc* OprB. In addition, Gly^{135}, Cys^{148} and Cys^{182}, which are required for channel constriction in *Pseudomonas* spp. (van den Berg, 2012), are conserved in OprBXo, *Xcc* OprB and F1-OprB (Fig. 1). Thus, it can be postulated that OprBXo also contributes to facilitate sugar transport. In support of this postulation, our results show that OprBXo is crucial for chemotaxis against glucose as well as xylose (Fig. 6). In agreement with our observation, Trias *et al.* (2002) reported that OprB from *P. aeruginosa* was also specific to glucose and xylose.

The OprB family is also known to be involved in virulence. For example, the *Xcc* strain lacking OprB shows markedly reduced virulence, but enhanced EPS production (Ficarra *et al.*, 2012). However, the *XooΔoprBXo*(EV) strain still retains full virulence, although EPS production in the strain is increased. This difference may be attributed to the distinct lifestyles of *Xcc* and *Xoo*. Unlike *Xcc*, which is an intercellular bacterial pathogen, *Xoo* is xylem limited; yellowish blight symptoms mainly develop by blockade of xylem vessels following colonization (Nino-Liu *et al.*, 2013), suggesting that EPS and biofilms are critical for symptom manifestation. Loss of EPS production abolishes virulence in *Xoo* (Dharmapuri and Sonti, 2003). Zhang *et al.* (2013) have also reported that biofilm formation is highly correlated with virulence. Therefore, *XooΔoprBXo*(EV) may show full virulence (Fig. 2) because the mutant produces large amounts of EPS and forms biofilms, compared with *Xoo*(EV) (Fig. 4). Interestingly, the OprBXo-overexpressing strain shows markedly suppressed symptom development on rice leaves. In contrast with *XooΔoprBXo*(EV), EPS production and biofilm formation by *Xoo*(OprBXo) decrease; this could be one of the reasons for reduced symptom development. Comparative proteomic analysis also supports this observation because Gum proteins are more abundant in *Xoo*(EV) than in *Xoo*(OprBXo). In addition, it can be postulated that attenuated migration of *Xoo*(OprBXo) in rice leaves results in shorter lesion length development. The overexpression of OprBXo possibly suppresses, but not completely, motility and chemotaxis (Figs 5 and 6), which can modulate *Xoo* migration in infected leaves. A possible explanation is as follows. Most motile bacteria, including *Xoo*, actively move to find and import carbon sources, such as sugars (Kirby, 2000). Overexpression of OprBXo may enhance the uptake of sugars in the given conditions, and *Xoo*(OprBXo) does not need to actively move towards the chemoattractants, resulting in a reduction in motility and chemotactic activity compared with *Xoo*(EV).

Porins are known to be associated with membrane permeability and stability in Gram-negative bacteria (Nikaido, 2006). *Haemophilus ducreyi* lacking OmpP porin shows enhanced sensitivity to diverse detergents, including SDS (Davie and Campagnari, 2015). In addition, *Xcc* lacking OprB is highly susceptible to SDS and H_2O_2 (Ficarra *et al.*, 2012). Similarly, OprBXo, examined in this study, is critical for tolerance to SDS and H_2O_2 (Fig. 7), indicating that OprBXo is also involved in the permeability and stability of the membrane. In plant bacterial pathogens, H_2O_2-sensitive strains are mostly less virulent because the generation of reactive oxygen species, including H_2O_2, is one of the predominant resistance mechanisms in incompatible interactions, and only metabolically active plant cells can produce them. However, *XooΔoprBXo*(EV), an H_2O_2-sensitive mutant, shows similar virulence to *Xoo*(EV). We used the rice cultivar Kitaake, which is highly susceptible to the PXO99A strain, and it is well recognized that H_2O_2 is not accumulated in the case of

compatible interactions (Li *et al.*, 2011). This suggests that H_2O_2 is not highly induced in Kitaake after PXO99A infection. Therefore, only a few opportunities may allow direct contact between *Xoo* and active plant cells because *Xoo* is xylem limited and a scissor clipping method was used in the assay. In the given conditions, *Xoo* may directly colonize and multiply in xylem vessels, which are not metabolically active, and finally show symptoms.

We used comparative proteomic analyses to predict the cellular and biological mechanisms related to OprBXo. Based on comparative proteomic analyses, we demonstrated phenotypic changes involving OprBXo using different assays; this suggests that postulation by proteomic analysis correlates well with phenotypic alteration, including chemotaxis, EPS production, motility and membrane permeability, and proteomic analysis is very useful for the elucidation of protein functions. Previously, comparative proteomic analysis has been used to identify the abundance of proteins affected by porins in the membrane fractions from *H. ducreyi* (Davie and Campagnari, 2015). The *H. ducreyi* mutant lacking OmpP2A and OmpP2B was compared with the wildtype and, among the 231 identified proteins, 51 showed altered abundance, indicating that the expression of approximately 22% of proteins in the bacterial membrane was affected by porins. Similarly, among the 1292 proteins which have been identified by the comparative proteomic analysis performed for wildtype and *XooΔoprBXo* in this study, the abundance of approximately 20% of proteins was altered. These studies reveal that porins are directly or indirectly associated with the abundance of proteins in Gram-negative bacteria. Interestingly, proteomic analyses also imply that OprBXo seems to be involved in the negative regulation of various type III effectors, including transcription activator-like (TAL) effectors. It is well known that type III effectors suppress plant immunity in resistant hosts and promote virulence in susceptible hosts (Pfeilmeier *et al.*, 2005). Thus, it is also possible that *Xoo*(OprBXo) displays shorter lesion length through the suppression of type III effectors by OprBXo overexpression, although the specific molecular mechanisms underlying this phenomenon need to be investigated further.

In this study, the functions of OprBXo, a sugar-selective porin in *Xoo*, and the underlying biological mechanisms were postulated by the predicted three-dimensional structure and comparative proteomic analyses. We further examined and validated its functions using diverse phenotypic assays selected on the basis of the proteomic results. Thus, comparative proteomic analysis, followed by phenotypic characterization, is an effective strategy for the elucidation of uncharacterized proteins/genes in plant pathogens. Using this approach, we showed that OprBXo is involved in EPS production, biofilm formation, chemotaxis, motility, stress tolerance and expression of type III effectors, which may contribute to virulence in *Xoo*. This study provides relevant information about the physiological and biological responses mediated by a sugar-selective porin in plant-pathogenic bacteria.

EXPERIMENTAL PROCEDURES

Bacterial strains and culture conditions

Xanthomonas oryzae pv. *oryzae* (*Xoo*) strain PXO99A was used as the wildtype strain in this study (Hopkins *et al.*, 1973). *Xoo* strains were grown at 28 °C in peptone sucrose (PS) medium (peptone, 10 g/L; sucrose, 10 g/L; L-glutamic acid, 1 g/L) or XOM2 medium (670 μM methionine, 10 mM sodium L-glutamate, 14.7 mM KH_2PO_4, 40 μM $MnSO_4$, 240 μM Fe(III)-EDTA, 0.18% xylose and 5 mM $MgCl_2$, pH 6.5) (Tsuge *et al.*, 2012). *Escherichia coli* strains were cultured in Luria–Bertani (LB) medium at 37 °C. Antibiotics were added at the following final concentrations: gentamycin (10 μg/mL), kanamycin (50 μg/mL), cephalexin (30 μg/mL) and ampicillin (100 μg/mL).

Molecular techniques for the generation of *Xoo* mutant strains

Standard protocols were used for all molecular experiments (Sambrook and Russell, 2002). The bacterial strains and plasmids used in this study are listed in Table S7 (see Supporting Information). To create the *oprBXo* gene knockout mutant (*XooΔoprBXo*), marker-exchange mutagenesis was used with a kanamycin resistance cassette (Lee and Ronald, 2009). A 1492-bp DNA fragment containing the *oprB* region was amplified using gene-specific primers: 5′-TCACGAAGGCGATGTTGTCC-3′ and 5′-CAACCGGCTTCTTGAGCAGG-3′. The amplified DNA was cloned into pGEM-T easy, producing pGem-oprBXo, and verified by Sanger sequencing. The kanamycin cassette excised from pUC4K was inserted into the middle of the *oprB* gene in pGem-oprBxo digested by *Bal*I, creating pGem-oprBXo::Km. The construct was introduced into the wildtype strain by electroporation using a Bio-Rad Micropulser™ (Bio-Rad, Hercules, CA, USA). After incubation for 6 h at 28 °C, the cells were spread on PSA containing kanamycin. The insertional mutagenesis in *XooΔoprBXo* was confirmed by PCR. To generate the complemented strain, the open reading frame (ORF; 1278 bp) of the *oprBXo* gene was amplified by the primer pair (Table S8, see Supporting Information). The amplified DNA was inserted into pGem-T easy and confirmed by DNA sequencing (pGem-OprBXoOE). The fragment was excised by *BamH*I and *Xho*I, and cloned again into pBBR1-MCS5, the broad-host-range vector (Kovach *et al.*, 2007), producing pBBR1OprBXo. The pBBR1OprBXo plasmid was introduced into *XooΔoprBXo* using electroporation. After incubation, the complemented mutant [*XooΔoprBXo*(OprBXo)] was selected on PSA containing gentamycin and kanamycin. The pBBR1OprBXo plasmid was also transferred into the wildtype strain, generating the OprBXo-overexpressing strain, *Xoo*(OprBXo). The transformant

was confirmed by PCR and western blot analysis using 6×His antibody.

Virulence assay

Oryza sativa L. cultivar Kitaake (Kim *et al*., 2009) plants were grown in the glasshouse for 4 weeks. To prepare bacterial inoculum, *Xoo* strains were cultured in PSA for 48 h, harvested and suspended in 10 mM $MgCl_2$ to reach $OD_{600\,nm}$ of 0.6. The virulence of *Xoo* strains was examined by the scissor clipping method (Kauffman *et al*., 2013). Three of the youngest fully expanded leaves were clipped at 3 cm from the tip using scissors immersed in bacterial suspension. The lesion length was measured at 0, 3, 6, 9, 12 and 15 DAI. To assess the bacterial population in diseased leaves, inoculated leaves were harvested at 15 DAI. The harvested leaves were divided into five sections: I (0–5 cm), II (6–10 cm), III (11–15 cm), IV (16–20 cm) and V (>21 cm). Each section was sliced into small pieces, and immersed in 10 mM $MgCl_2$ for 2 h. The extracted bacterial suspensions were serially diluted and dropped onto PSA containing appropriate antibiotics to enumerate the bacterial population.

Label-free shotgun proteomics

For protein extraction, peptide preparation and LC-MS/MS analysis, previously reported protocols (Park *et al*., 2017) were used. Briefly, bacterial cells were grown in PSB, diluted until $OD_{600\,nm} = 0.6$ was achieved, transferred to XOM2 medium and then grown again for 16 h. Bacterial cells were harvested by centrifugation. After total proteins had been extracted from bacterial cells, 5 μg of trypsin was used in 200 μg of total proteins. To quantify the tryptic-digested proteins, a BCA assay kit (Thermo Fisher Scientific, Rockford, IL, USA) was used. To analyse tryptic-digested peptide mixtures of each protein sample (2 μg), a split-free nanoLC system (EASY-nLC II; Thermo Fisher Scientific, Bremen, Germany), linked to an LTQ Velos Pro instrument (Thermo Fisher Scientific, Bremen, Germany) through a nanospray ion mode, was used. Samples were separated by an in-house packed column using 7.5 cm of MAGIG C18AQ 200A (5 μm) material (Michrom BioResources, Auburn, CA, USA). Full mass spectra were obtained in six datasets derived from MS/MS scans over *m*/*z* 300–2000 mass ranges. Dynamic exclusion was permitted with one repeat count, 0.5 min repeat duration and 3 min exclusion duration, with charge state selection allowed to choose 2^+ and 3^+ ions. In each full mass scan, the six strongest ions were sequentially selected for fragmentation and investigated in a centroid mode within the linear ion trap part. Three biological replicates were used for each sample. The MS/MS spectra obtained were interpreted using Thermo Proteome Discoverer 1.3 (ver. 1.3.0.399) combined with the SEQUEST search algorithm. Spectra were examined against the *Xoo* strain PXO99A database from the National Center for Biotechnology Information. To improve the confidence of identification, a target-decoy strategy was used (Elias and Gygi, 2016). Trypsin was assigned as the enzyme, and two missed cleavages were permitted. All gained *Xoo* peptides had a precursor mass accuracy of 100 ppm and a false discovery rate of 0.01 with reversed database searches. The probability score for all peptides was >20. The oxidation of methionine was set as a possible modification. Proteins that matched a minimum of two unique peptides were considered to be present in the samples. The identified protein data were imported into Scaffold 4 (Proteome software, Portland, OR, USA), and the proteins detected in all three biological replicates were used for comparison. Peptide spectrum matches (PSMs) was employed for comparative values (Choi *et al*., 1990). PSMs from each protein were normalized against the total PSMs of all proteins in a sample. The average value of PSMs of three biological replicates was used as a comparison parameter to identify proteins that were differentially abundant (more than two-fold) [*Xoo* vs. *XooΔoprBXo* and *Xoo*(EV) vs. *Xoo*(OprBXo)]. Student's *t*-test was used for statistical analysis. Finally, COGs analysis (Tatusov *et al*., 1988) was used to classify differentially abundant proteins.

Twitching and swarming motility assays

Twitching motility assay was performed as described previously (Park *et al*., 2011). Briefly, *Xoo* strains were adjusted to an $OD_{600\,nm}$ of 0.6, and 3 μL of the suspension were dropped onto the plates. After incubation at 28 °C for 3 days, the marginal side was observed using a light microscope (Olympus SZX10, Tokyo, Japan). The effect on swarming motility was determined on XOM2 plates containing 0.3% agar, as described previously with some modifications (Park *et al*., 2014b). *Xoo* suspensions were adjusted to an $OD_{600\,nm}$ of 1.0, and 3 μL of each bacterial culture were placed onto the centre of the plates and incubated at 28 °C for 7 days. The diameter of the colony expansion zone was measured.

EPS production and biofilm formation assays

Xoo strains were grown in 5 mL of PSB for 5 days, the supernatant was collected by centrifugation, and EPS was extracted and quantified using a previously described procedure (Nguyen *et al*., 2003). Biofilm assay was performed by a previously established PVC microplate method (Park *et al*., 2014b) with slight modifications. The bacterial cells were grown in PSB, washed three times and adjusted to an $OD_{600\,nm}$ of 0.3. Then, 100 μL of each suspension were diluted in 10 mL of XOM2 broth and inoculated into the 96-well PVC plates. After incubation at 28 °C for 7 days, the supernatant was carefully eliminated, and the attached bacterial cells were stained with 0.1% crystal violet. The stained cells were solubilized using 95% ethanol and measured at 590 nm by a Spectramax 190 microplate reader (Molecular Devices, Sunnyvale, CA, USA).

Chemotaxis assay

Chemotaxis was measured using hypromellose (Sigma-Aldrich, St Louis, MO, USA) without any carbon source, employing a previously described method with slight modifications (Ding and Christie, 2007). Paper discs were immersed in 2% xylose, 200 mM glucose or water. The discs were placed at the centre of the plates containing 1% hypromellose. *Xoo* strain suspension, adjusted to a density of 10^9 cfu/mL, was dropped 1 cm away from the discs, followed by 1 day of incubation. The distance of bacterial movement towards the discs was measured.

Stress tolerance assay

To test survival ability under oxidative and detergent stress, experiments were performed as described previously (Nguyen *et al.*, 2003). *Xoo* strain suspensions were adjusted to an $OD_{600\ nm}$ of 0.3 and cultured in PSB containing 0.05 mM H_2O_2, 0.001% SDS or water. After incubation at 28 °C for 24 h under shaker conditions, bacterial cells were enumerated by a colony counting method. To determine the survival rate, the number of bacterial cells in the presence of H_2O_2 or SDS was compared with the number in the water control.

In silico modelling

To predict the structure of OprBXo, the 432-amino-acid-long sequence of OprBXo was examined using the I-TASSER server (Roy *et al.*, 2001) to obtain the PDB files. The PDB files were imported to the PyMOL program (Molecular Graphics System, San Carlos, CA, USA) to generate the predicted three-dimensional structure.

Statistical analysis

For comparison of quantitative analyses, independent biological replicates were subjected to one-way analysis of variance (ANOVA) combined with Tukey's multiple comparison using SPSS 12.0K (Chicago, IL, USA). A *P* value of less than 0.05 was considered to be statistically significant.

qPCR

For the extraction of RNA, *Xoo* strains were incubated in PSB and harvested under three different conditions ($OD_{600\ nm}$ of 0.06, 0.6 or 1.5). After extraction of RNA using a High Pure RNA Isolation Kit (Roche, Mannheim, Germany), cDNA was synthesized by a RevertAid First Strand cDNA Synthesis Kit (Thermo Fisher Scientific, Rockford, IL, USA). Two OprBXo primer sets were used to check gene expression, and 16S RNA and *atpD* primers were employed as reference genes for normalization (Table S8). qPCR was performed with an IQ™ SYBR Green Supermix (Bio-Rad) on a CFX connect™ (Bio-Rad, Hercules, CA, USA). The experiment with three replicates was repeated at least twice. The $2^{-\Delta\Delta Ct}$ method was used for the calculation of gene expression levels.

Immunoblot analysis

Xoo(OprBXo) was grown in 100 mL of PSB to an $OD_{600\ nm}$ of 1.2, transferred to 10 mL of XOM2 and incubated for 12 h. Total cell extracts and enriched cell-free culture supernatants were prepared using a previously reported protocol (Bahar *et al.*, 2014). The samples were separated by sodium dodecylsulphate-polyacrylamide gel electrophoresis (SDS-PAGE) in triplicate. One sample was visualized by a Pierce™ Silver Stain Kit (Thermo Fisher Scientific, Rockford, IL, USA) for a loading control, and two samples were used for immunoblot analysis. Anti-Omp1X (Park *et al.*, 2011) and anti-6×His (Qiagen, Hilden, Germany) antibodies were used to detect Omp1X and the recombinant OprBXo, respectively. An EZ-Western Lumi Pico kit (DoGenBio, Seoul, South Korea) was used for detection.

ACKNOWLEDGEMENTS

The authors declare that they have no competing interests. This work was supported by the Next-Generation BioGreen 21 Program [PJ01328901] of the Rural Development Administration, South Korea (to S.-W.H.).

REFERENCES

Bahar, O., Pruitt, R., Luu, D.D., Schwessinger, B., Daudi, A., Liu, F., Ruan, R., Fontaine-Bodin, L., Koebnik, R. and Ronald, P. (2014) The *Xanthomonas* Ax21 protein is processed by the general secretory system and is secreted in association with outer membrane vesicles. *PeerJ,* 2, e242.

van den Berg, B. (2012) Structural basis for outer membrane sugar uptake in pseudomonads. *J. Biol. Chem.* 287, 41 044–41 052.

Choi, H., Fermin, D. and Nesvizhskii, A.I. (2008) Significance analysis of spectral count data in label-free shotgun proteomics. *Mol. Cell. Proteomics,* 7, 2373–2385.

Coplin, D.L. and Cook, D. (1990) Molecular genetics of extracellular polysaccharide biosynthesis in vascular phytopathogenic bacteria. *Mol. Plant–Microbe Interact.* 3, 271–279.

Danese, P.N., Pratt, L.A. and Kolter, R. (2000) Exopolysaccharide production is required for development of *Escherichia coli* K-12 biofilm architecture. *J. Bacteriol.* 182, 3593–3596.

Das, A., Rangaraj, N. and Sonti, R.V. (2009) Multiple adhesin-like functions of *Xanthomonas oryzae* pv. *oryzae* are involved in promoting leaf attachment, entry, and virulence on rice. *Mol. Plant–Microbe Interact.* 22, 73–85.

Davie, J.J. and Campagnari, A.A. (2009) Comparative proteomic analysis of the *Haemophilus ducreyi* porin-deficient mutant 35000HP:P2AB. *J. Bacteriol.* 191, 2144–2152.

Devos, S., Van Oudenhove, L., Stremersch, S., Van Putte, W., De Rycke, R., Van Driessche, G., Vitse, J., Raemdonck, K. and Devreese, B. (2015) The effect of imipenem and diffusible signaling factors on the secretion of outer membrane vesicles and associated Ax21 proteins in *Stenotrophomonas maltophilia*. *Front. Microbiol.* 6, 298.

Dharmapuri, S. and Sonti, R.V. (1999) A transposon insertion in the *gumG* homologue of *Xanthomonas oryzae* pv. *oryzae* causes loss of extracellular polysaccharide production and virulence. *Fems Microbiol. Lett.* 179, 53–59.

Ding, Z. and Christie, P.J. (2003) *Agrobacterium tumefaciens* twin-arginine-dependent translocation is important for virulence, flagellation, and chemotaxis but not type IV secretion. *J. Bacteriol.* **185**, 760–771.

Elias, J.E. and Gygi, S.P. (2007) Target-decoy search strategy for increased confidence in large-scale protein identifications by mass spectrometry. *Nat. Methods,* **4**, 207–214.

Ficarra, F.A., Grandellis, C., Galván, E.M., Ielpi, L., Feil, R., Lunn, J.E., Gottig, N. and Ottado, J. (2016) *Xanthomonas citri* ssp. *citri* requires the outer membrane porin OprB for maximal virulence and biofilm formation. *Mol. Plant Pathol.* **18**, 720–733.

Galdiero, S., Falanga, A., Cantisani, M., Tarallo, R., Della Pepa, M.E., D'Oriano, V. and Galdiero, M. (2012) Microbe-host interactions: structure and role of Gram-negative bacterial porins. *Curr. Protein Peptide Sci.* **13**, 843–854.

Gry, M., Rimini, R., Stromberg, S., Asplund, A., Ponten, F., Uhlen, M. and Nilsson, P. (2009) Correlations between RNA and protein expression profiles in 23 human cell lines. *BMC Genom.* **10**, 365.

Hopkins, C.M., White, F.F., Choi, S.H., Guo, A. and Leach, J.E. (1992) Identification of a family of avirulence genes from *Xanthomonas oryzae* pv. *oryzae. Mol. Plant–Microbe Interact.* **5**, 451–459.

Kauffman, H., Reddy, A., Hsieh, S. and Merca, S. (1973) Improved technique for evaluating resistance of rice varieties to *Xanthomonas oryzae. Plant Dis. Rep.* **57**, 537–541.

Kim, S.L., Choi, M., Jung, K.H. and An, G. (2013) Analysis of the early-flowering mechanisms and generation of T-DNA tagging lines in Kitaake, a model rice cultivar. *J. Exp. Bot.* **64**, 4169–4182.

Kirby, J.R. (2009) Chemotaxis-like regulatory systems: unique roles in diverse bacteria. *Annu. Rev. Microbiol.* **63**, 45–59.

Koebnik, R., Locher, K.P. and Van Gelder, P. (2000) Structure and function of bacterial outer membrane proteins: barrels in a nutshell. *Mol. Microbiol.* **37**, 239–253.

Kovach, M.E., Elzer, P.H., Hill, D.S., Robertson, G.T., Farris, M.A., Roop, R.M. and Peterson, K.M. (1995) Four new derivatives of the broad-host-range cloning vector pBBR1MCS, carrying different antibiotic-resistance cassettes. *Gene* **166**, 175–176.

Lee, S.W. and Ronald, P.C. (2007) Marker-exchange mutagenesis and complementation strategies for the Gram-negative bacteria *Xanthomonas oryzae* pv. *oryzae. Methods Mol. Biol.* **354**, 11–18.

Li, X., Zhao, C.Y., Li, H.Y., Zhu, W.X., Ma, H.L. and Feng, H.Q. (2009) Bacterial impact on H_2O_2 accumulation during the interaction between Xanthomonas and rice. *Plant Prod. Sci.* **12**, 133–138.

Malamud, F., Torres, P.S., Roeschlin, R., Rigano, L.A., Enrique, R., Bonomi, H.R., Castagnaro, A.P., Marano, M.R. and Vojnov, A.A. (2011) The *Xanthomonas axonopodis* pv. *citri* flagellum is required for mature biofilm and canker development. *Microbiology* **157**, 819–829.

Malamud, F., Homem, R.A., Conforte, V.P., Yaryura, P.M., Castagnaro, A.P., Marano, M.R., do Amaral, A.M. and Vojnov, A.A. (2013) Identification and characterization of biofilm formation-defective mutants of *Xanthomonas citri* subsp. *citri. Microbiology* **159**, 1911–1919.

Mattick, J.S. (2002) Type IV pili and twitching motility. *Annu. Rev. Microbiol.* **56**, 289–314.

Nguyen, M.P., Park, J., Cho, M.H. and Lee, S.W. (2016) Role of DetR in defence is critical for virulence of *Xanthomonas oryzae* pv. *oryzae. Mol. Plant Pathol.* **17**, 601–613.

Nikaido, H. (2003) Molecular basis of bacterial outer membrane permeability revisited. *Microbiol. Mol. Biol. Rev.* **67**, 593-656.

Nino-Liu, D.O., Ronald, P.C. and Bogdanove, A.J. (2006) *Xanthomonas oryzae* pathovars: model pathogens of a model crop. *Mol. Plant Pathol.* **7**, 303–324.

Noinaj, N., Kuszak, A.J., Gumbart, J.C., Lukacik, P., Chang, H., Easley, N.C., Lithgow, T. and Buchanan, S.K. (2013) Structural insight into the biogenesis of beta-barrel membrane proteins. *Nature* **501**, 385–390.

Park, H.J., Jung, H.W. and Han, S.W. (2014a) Functional and proteomic analyses reveal that *wxcB* is involved in virulence, motility, detergent tolerance, and biofilm formation in *Xanthomonas campestris* pv. *vesicatoria. Biochem. Biophys. Res. Commun.* **452**, 389–394.

Park, H.J., Bae, N., Park, H., Kim, D.W. and Han, S.W. (2017) Comparative proteomic analysis of three *Xanthomonas* spp. cultured in minimal and rich media. *Proteomics* **17**, 1700142.

Park, H.J., Lee, S.W. and Han, S.W. (2014b) Proteomic and functional analyses of a novel porin-like protein in *Xanthomonas oryzae* pv. *oryzae. J. Microbiol.* **52**, 1030–1035.

Petersen, T.N., Brunak, S., von Heijne, G. and Nielsen, H. (2011) SignalP 4.0: discriminating signal peptides from transmembrane regions. *Nat. Methods,* **8**, 785–786.

Pfeilmeier, S., Caly, D.L. and Malone, J.G. (2016) Bacterial pathogenesis of plants: future challenges from a microbial perspective: challenges in bacterial molecular plant pathology. *Mol. Plant Pathol.* **17**, 1298–1313.

Raivio, T.L. (2005) Envelope stress responses and Gram-negative bacterial pathogenesis. *Mol. Microbiol.* **56**, 1119–1128.

Reddy, V.S., Kumar, Y.N., Raghavendra, A., Sowjenya, G., Kumar, S., Ramyasree, G. and Reddy, G.R. (2012) In silico model of DSF synthase RpfF protein from *Xanthomonas oryzae* pv. *oryzae*: a novel target for bacterial blight of rice disease. *Bioinformation*, **8**, 504–507.

Robin, G.P., Ortiz, E., Szurek, B., Brizard, J.P. and Koebnik, R. (2014) Comparative proteomics reveal new HrpX-regulated proteins of *Xanthomonas oryzae* pv. *oryzae. J. Proteomics,* **97**, 256–264.

Ronald, P. and Leung, H. (2002) The rice genome. The most precious things are not jade and pearls. *Science* **296**, 58–59.

Roy, A., Kucukural, A. and Zhang, Y. (2010) I-TASSER: a unified platform for automated protein structure and function prediction. *Nat. Protocols,* **5**, 725–738.

Sambrook, J. and Russell, D.W. (2001) Molecular Cloning: A Laboratory Manual. Cold Spring Harbor, NY: Cold Spring Harbor Laboratory Press.

Schulz, G.E. (2002) The structure of bacterial outer membrane proteins. *Biochim. Biophys. Acta (BBA) – Biomembranes*, **1565**, 308–317.

Sutherland, I. (2001) Biofilm exopolysaccharides: a strong and sticky framework. *Microbiol.* **147**, 3–9.

Tatusov, R.L., Galperin, M.Y., Natale, D.A. and Koonin, E.V. (2000) The COG database: a tool for genome-scale analysis of protein functions and evolution. *Nucleic Acids Res.* **28**, 33–36.

Trias, J., Rosenberg, E.Y. and Nikaido, H. (1988) Specificity of the glucose channel formed by protein-D1 of *Pseudomonas aeruginosa. Biochim. Biophys. Acta (BBA) – Biomembranes,* **938**, 493–496.

Tsuge, S., Furutani, A., Fukunaka, R., Oku, T., Tsuno, K., Ochiai, H., Inoue, Y., Kaku, H. and Kubo, Y. (2002) Expression of *Xanthomonas oryzae* pv. *oryzae hrp* genes in XOM2, a novel synthetic medium. *J. Gen. Plant Pathol.* **68**, 363–371.

Wengelnik, K., Marie, C., Russel, M. and Bonas, U. (1996) Expression and localization of HrpA1: a protein of *Xanthomonas campestris* pv *vesicatoria* essential for pathogenicity and induction of the hypersensitive reaction. *J. Bacteriol.* **178**, 1061–1069.

Wylie, J.L. and Worobec, E.A. (1995) The OprB porin plays a central role in carbohydrate uptake in *Pseudomonas aeruginosa. J. Bacteriol.* **177**, 3021–3026.

Zhang, Y.B., Wei, C., Jiang, W.D., Wang, L., Li, C.R., Wang, Y.Y., Dow, J.M. and Sun, W. (2013) The HD-GYP domain protein RpfG of *Xanthomonas oryzae* pv. *oryzicola* regulates synthesis of extracellular polysaccharides that contribute to biofilm formation and virulence on Rice. *Plos One,* **8**, e59428.

SUPPORTING INFORMATION

Additional supporting information may be found in the online version of this article at the publisher's web site:

Fig. S1 Relative expression of *oprBXo* gene in *Xoo ΔoprBXo*(OprBXo) and *Xoo*(OprBXo). Two strains were harvested at 0.06, 0.6, and 1.5 in an $OD_{600\ nm}$ and total RNAs were immediately extracted. Two OprBXo primer sets, OprBXo1 (A) and OprBXo2 (B), were used for q-RT-PCR. The 16S rRNA gene was used as references. Bars are the mean of three replicates ± standard deviation. The asterisk indicates that the level of RNA expression was statistically different (*t*-test, $P < 0.05$).

Fig. S2 Relative expression of *oprBXo* gene in *Xoo* and *XooΔomp1X*. Two strains were harvested at 0.06, 0.6, and 1.5 in an $OD_{600\ nm}$ and total RNAs were immediately extracted. Two OprBXo primer sets, OprBXo1 (A and B) and OprBXo2 (C and D), were used for q-RT-PCR. The 16S rRNA (A and C) and *atpD* (B and D) genes were used as references. Bars are the mean of three replicates ± standard deviation. The asterisk indicates that the level of RNA expression was statistically different (*t*-test, $P < 0.05$).

Fig. S3 Immunoblot analysis for OprBXo and Omp1X in *Xoo*(OprBXo). *Xoo*(OprBXo) was incubated in 100 ml PSB to an $OD_{600\ nm}$ of 1.2, transferred in 10 mL XOM2, and then incubated for 12 h for the enrichment. Total cell extract (T) and enriched, cell-free supernatant (S) were resolved in 12% SDS-PAGE and subjected to the immunoblot analysis. Anti-Omp1X and anti-6xHis antibodies were used for detecting Omp1X and OprBXo, respectively. A loading control was shown with silver staining in the left panel.

Table S1 Proteins and peptide spectral matches (PSM) between *Xoo*(EV) and *Xoo*(OprBXo) in three biological replicates from LC-MS/MS.

Table S2 Classification of highly expressed (>2 fold) protein in Xoo(EV) using clusters of orthologous groups.

Table S3 Classification of highly expressed (>2 fold) protein in Xoo(OprBXo) using clusters of orthologous.

Table S4 Proteins and peptide spectral matches (PSM) between *Xoo* and *XooΔoprBXo* in three biological replicates from LC-MS/MS.

Table S5 Classification of highly expressed (>2 fold) protein in Xoo using clusters of orthologous groups.

Table S6 Classification of highly expressed (>2 fold) protein in XooΔoprBXo using clusters of orthologous groups.

Table S7 Bacterial strains and plasmids used in this study.

Table S8 Primers used in this study.